

Aperture Synthesis Observations of Galactic H II Regions

III. Small H II Regions in the Anticenter Region

F. P. Israel

Sterrewacht, Huygens Laboratorium, Wassenaarseweg 78, Leiden 2403, The Netherlands

Received December 23, 1975, revised May 24, 1976

Summary. Aperture Synthesis Observations at wavelengths of 6 and 21 cm of the H II regions, S 254, S 255, S 256, S 257, S 258, S 266, S 269, S 271 and S 272 are presented. The observations show:

1. Most of the observed H II regions are completely resolved at λ 6 cm. Thus any structure on a scale smaller than 0.05 pc contributes only a very small amount to the total flux density of the source.

2. The mass of the exciting stars appears to be at least an order of magnitude larger than the mass of the ionized gas. The ionized mass of most regions is of the order of $1 M_{\odot}$ or less.

3. None of the observed H II regions is excited by a star of spectral type earlier than O9.5. Most regions have r.m.s. electron-densities of $100\text{--}300 \text{ cm}^{-3}$.

4. The group of H II regions S 254–S 258 probably indicates an early stage of a new OB cluster containing at least seven early type B stars in an area 3 pc across.

5. Between the regions S 255 and S 257 an optically thick, compact H II region is found. Its position is near, but not coincident with that of an OH/H₂O maser. Near the radiopeak of S 269 an OH/H₂O maser is present. The two do not coincide.

6. The central exciting stars of S 256, S 266 and S 271 are located in “holes” of low radio surface brightness.

Key words: aperture synthesis radio observations — H II regions — star formation

I. Introduction

This paper is the third in a series dealing with high resolution observations of galactic H II regions using the Westerbork Synthesis Radio Telescope (WSRT). In the first paper (Israel et al., 1973, paper I) λ 21 cm observations of a number of small H II regions in the Perseus Arm around $l = 111^{\circ 1}$ was discussed; the second

paper (Israel, 1976, Paper II) dealt with the strong and complex galactic source W 58 at $l = 70^{\circ} 5$. In this Paper I present observations at λ 6 cm and λ 21 cm of the H II regions S 254, S 255, S 256, S 257, S 258, S 266, S 271 and S 272. A study of these nebulae at radio frequencies is of interest for a number of reasons. They are optically well studied (Chopin et al., 1973, 1974); they all seem to be excited by only one OB star each; they are all fairly isolated regions with little obscuration, and none of them is part of a confusing large complex. Both S 255 and S 269 are associated with OH and H₂O masers (Turner, 1971; Lo and Burke, 1973). Particularly of interest are the ratio of the mass of the exciting stars to the mass of the ionized region, especially in view of the general question how much mass is left over in the process of star formation. Therefore one also wants to know whether these regions are photon-limited or mass-limited, and the velocity of the star relative to the gas.

In order to calculate physical parameters from the observed parameters one needs to know the distances of the regions. Unfortunately, these are poorly known. Georgelin et al. (1973) note a large discrepancy between distances derived from H α radial velocities and those derived from the characteristics of the exciting stars. The radial velocity data are summarized in Table 1.

The kinematical distances are calculated according to the model by Schmidt (1965). Throughout this article I adopt the following distances: for S 254–S 258 $D = 1.25$ kpc; for S 266 $D = 1.5$ kpc; for S 269, S 271 and S 272 $D = 2$ kpc. It is necessary to keep in mind that the distances in reality may be as high as 3 kpc. The derived mass of the H II region which is proportional to the distance to the power 2.5 will be most strongly influenced by this uncertainty while the emission measure is independent of it. Previous (mostly single dish) radio observations are summarized in Table 2. In general, the nebulae are too small to be resolved by the instruments used. The observed spectra all appear to be thermal and optically thin.

The observations of S 266 are conflicting; this is caused by confusion with two strong non-thermal

¹ Throughout this paper, l and b represent new galactic coordinates l^{II} and b^{II}

Table 1. Radial velocities and distances

Line	Name	Velocity (LSR) (km s ⁻¹)	Kin. dist. (kpc)	Opt. dist. (kpc)	Reference
(1)	(2)	(3)	(4)	(5)	(6)
H α	S 254	+ 6.6 \pm 0.9	1.1	3.2	Georgelin et al. (1973)
H α	S 255	+ 5.3 \pm 0.9	0.8	—	Georgelin et al. (1973)
H α	S 255	+ 8.9 \pm 3.6	1.3	—	Miller (1968)
OH 1665 emission	S 255	+ 6	0.9	—	Turner (1971)
CS	S 255	+ 8.3	1.3	—	Morris et al. (1974)
CO	S 255	+ 7.8	1.2	—	Blair et al. (1975)
H ₂ O	—	+ 8.2; + 15.0	1.3–2.3	—	Lo and Burke (1973)
CO	S 256	+ 7.1	1.1	—	Blair et al. (1975)
H α	S 257	+ 7.8 \pm 3.6	1.2	3.2	Georgelin et al. (1973)
H α	S 269	+ 13.6	1.7	—	Georgelin et al. (1973)
OH 1665 emission	S 269	+ 14; + 17	1.7–2.0	—	Turner (1971)
H ₂ O	S 269	+ 16.5; + 18.7	2.0–2.3	—	Lo and Burke (1973)
CO	S 269	+ 17	2.0	—	Wilson et al. (1974)
					Blair et al. (1975)
H α	S 271	+ 16.6	1.9	—	Georgelin et al. (1973)

Table 2. Previous radio observations

Name	Freq. (MHz)	HPBW (arc min)	Flux density (f.u.)	Reference
(1)	(2)	(3)	(4)	(5)
S 254, S 255, S 256, S 257, S 258	178	23	5 \pm 1	Caswell (1970)
	318	16.2	4.0 \pm 1.0	Terzian (1970)
	606	9	7.8 \pm 2	Terzian and Pankonin (1972)
	610	16 \times 22	4.2 \pm 0.5	Dickel et al. (1967)
	635	31	6 \pm 2	Milne and Hill (1969)
	1410	15	5 \pm 1	Milne and Hill (1969)
	2650	8.4	4.9 \pm 0.5	Milne and Hill (1969)
	2700	8.2	3.2 \pm 0.3	Day et al. (1972)
S 255	4850	1.5 \times 7	1.82	Kazès et al. (1975)
	15500	2.2	0.77 \pm 0.10	Johnson (1974)
S 257	4850	1.5 \times 7	0.5	Kazès et al. (1975)
S 266	408	3 \times 10	0.20 \pm 0.03	Ficarra and Padrielli (1968)
	430	10	2.00 \pm 0.50	Terzian (1966)
	610	16 \times 22	3.5 \pm 0.5	Dickel et al. (1967)
	2700	8.2	2.0 \pm 0.5	Day et al. (1972)
	2840	—	0.18 \pm 0.05	Thompson and Colvin (1967)
	3240	8.4	0.32 \pm 0.078	Higgs (1971)
	4850	1.5 \times 7	0.1	Kazès et al. (1975)
	4995	—	0.20 \pm 0.5	Kaftan-Kassim (1968)
	6630	4.0	0.131 \pm 0.033	Higgs (1971)
	7875	4.4	0.15 \pm 0.05	Johnson (1974)
	10630	2.7	0.147 \pm 0.057	Higgs (1971)
	10700	1.6	0.056 \pm 0.005	Altenhoff et al. (1973)
	15370	2	-0.04 \pm 0.55	Rubin (1970)
	15500	2.2	0.18 \pm 0.18	Johnson (1974)
S 269	318	16.2	0.8 \pm 0.2	Terzian (1970)
	606	9	0.7 \pm 0.2	Terzian and Pankonin (1972)
	1400	10	0.8 \pm 0.1	Felli and Churchwell (1972)
	1416	4 \times 22	0.71	Kazès et al. (1975)
	2700	8.2	0.7 \pm 0.15	Day et al. (1972)
	2695	11.2	1.1 \pm 0.7	Churchwell and Felli (1970)
	4850	1.5 \times 7	1.05	Kazès et al. (1975)
S 271, S 272	1400	10	0.3	Felli and Churchwell (1972)
	1416	4 \times 22	0.22	Kazès et al. (1975)
	2695	11.2	1.4 \pm 0.7	Churchwell and Felli (1970)
	2695	2.2 \times 11	0.22	Kazès et al. (1975)
	2700	8.2	0.4 \pm 0.15	Day et al. (1972)
	4850	1.5 \times 7	0.40	Kazès et al. (1975)
	7875	4.4	0.18 \pm 0.03	Johnson (1974)

point sources nearby (see Section III-8). The confused situation with S 271 and S 272 is likewise caused by the presence of nearby non-thermal background sources.

II. Observations

All observations were carried out with the Westerbork Synthesis Radio Telescope, operating at frequencies of 1415 MHz and 4995 MHz. The instrument is described in detail by Baars and Hooghoudt (1974) and Casse and Muller (1974). Details relevant to the present observations are given in Table 3 and 4.

The observations were reduced using the standard procedures (Högbom and Brouw, 1974; van Someren Gréve, 1974; Ekers et al., 1973).

i) Because of the low declination of the observed sources, telescopes shadowed each other at the extreme hour-angles; they also reflected strong emission into each other ("cross-talk"). These effects are most serious between telescopes 9 and A, that together form the shortest spacing of 36 m.

For this reason, emission observed by these two telescopes at extreme hour angles (usually between -90° and -60° , and between $+60^\circ$ and $+90^\circ$) was not included in the maps.

ii) At λ 21 cm the relatively bright regions S 255, S 256 and S 257 are severely distorting the low-brightness structure of S 254; at λ 6 cm the relatively bright region S 255 is interfering with the less bright H II regions S 256 and S 257. In both maps I used the clean procedure (Högbom, 1974) to eliminate the disturbing sources from the maps; they were later restored using only the center of the synthesized beam.

In Table 5 all observed H II regions are listed; other sources detected in the observed fields are listed in Table 6.

Table 3. WSRT parameters

Frequency (MHz)	1415	4995
Wavelength (cm)	21.2	6.0
HPBW Primary Beam (arc min)	37.6	12
HPBW Synthesized Beam (arc s)	$24.6 \times 24.6 \text{ cosec } \delta$	$7.2 \times 7.2 \text{ cosec } \delta$
r.m.s. Noise per 1×12 h (m.f.u. per beam)	1.2	1.3
HPW of a gaussian source with fringe amplitude 0.5 at 36 m spacing (arc min)	$9 \times 9 \text{ cosec } \delta$	$2.5 \times 2.5 \text{ cosec } \delta$

The flux-densities S in Table 5 were all determined by planimetry of the contour maps. Their estimated accuracy is about 15%. They are corrected for primary beam sensitivity decreases. Positions and sizes were all determined from the contourmaps. The (gaussian) sizes θ_G are corrected for finite beamwidth.

In Table 6 the positions and flux densities marked with an asterisk were found by the standard search program. For the other sources they were determined from line plots. The flux densities in Table 6 are peak values and therefore lower limits to the actual flux densities. Since most sources do not show any beam broadening, the error will be small.

III. Results on Individual H II Regions

1. Physical Parameters

Mezger and Henderson (1967) give equations that I used to derive the physical parameters in Table 7 from the observed quantities given in Table 5. The derived parameters are those of a model H II region, consisting of pure hydrogen homogeneously distributed in a cylinder whose depth equals its diameter d . Thus the

Table 4. Observations log

Field	Date	Duration	Fieldcenter	Range of interferom. spacings (m)	Increment (m)
(1)	(2)	(3)	(4)	(5)	(6)
Observations at λ 21 cm					
S 254	July 1971	1×12 h	$06^{\text{h}}09^{\text{m}}00^{\text{s}}$ $18^{\circ}00'00''$	36-1404	72
S 269	Feb. 1972	1×12 h	$06^{\text{h}}12^{\text{m}}00^{\text{s}}$ $13^{\circ}51'00''$	36-1404	72
S 271	Feb./March 1972	1×12 h	$06^{\text{h}}12^{\text{m}}00^{\text{s}}$ $12^{\circ}22'12''$	36-1404	72
Observations at λ 6 cm					
S 255	July 1973	1×12 h	$06^{\text{h}}10^{\text{m}}00^{\text{s}}$ $18^{\circ}00'00''$	36-1404	72
S 266	May 1974	1×12 h	$06^{\text{h}}16^{\text{m}}00^{\text{s}}$ $15^{\circ}18'00''$	36-1440	36
S 269	Feb. 1973	1×12 h	$06^{\text{h}}12^{\text{m}}00^{\text{s}}$ $13^{\circ}51'00''$	36-1404	72
S 271	July 1973	1×12 h	$06^{\text{h}}12^{\text{m}}12^{\text{s}}$ $12^{\circ}22'12''$	36-1404	72

Table 5. Observed parameters

Name	Right ascension (1950.0)	Declination (1950.0)	Gal. long. <i>l</i>	Gal. lat. <i>b</i>	Flux-density		Equiv. Gaussian Diam. (arc min)
					S_{1415} (f.u.)	S_{4995} (f.u.)	
(1)	(2)	(3)	(4)	(5)	(6)	(7)	(8)
S 254	06 ^h 09 ^m 25 ^s	18°02'00"	192.51	-0.15	1.8	not observed	7.5 × 10.0 (8.7)
S 256	06 09 41.5	17 57 42	192.60	-0.13	0.130	0.150	0.9 × 1.9 (0.9)
S 257	06 09 49.2	18 00 00	192.58	-0.08	0.550	0.500	1.8 × 2.3 (2.0)
G 192.58-0.04	06 09 58.04	18 01 17.1	192.58	-0.04	0.014	0.023	≤ 0.05
G 192.60-0.04	06 09 59.66	18 00 16.2	192.60	-0.04	—	0.008	0.14
S 255	06 10 09	17 59 30	192.63	-0.02	1.8	1.7	2.1 × 2.3 (2.2)
S 258	06 10 35	17 55 42	192.74	-0.04	≤ 0.025	not observed	0.6 ^a
S 269 total	06 11 47.0	13 51 00	196.45	-1.67	0.660	0.600	1.6 × 2.3 (1.9)
S 269 A	06 11 47.0	13 51 00	196.45	-1.67	—	0.125	0.3
S 271	06 12 05.0	12 22 12	197.78	-2.32	0.260	0.240	1.1 × 1.1 (1.05)
S 272	06 12 13.2	12 20 00	197.83	-2.31	0.005	not observed	0.2 ^a
S 266	06 15 54.0	15 18 48	195.64	-0.10	not observed	0.080	0.9

^a Optical Diameters**Table 6.** Other sources detected

Source number	Field	Right ascension (1950.0)	Declination (1950.0)	Flux-density		Remarks
				S_{1415} (m.f.u.)	S_{4995} (m.f.u.)	
1*	S 254	06 ^h 08 ^m 47 ^s .1	17°51'29"	330	—	
2*	S 254	06 08 59	18 16 34	14	—	
3*	S 269	06 09 44.5	13 57 57	130	—	
4*	S 255	06 09 47.3	18 02 47.3	—	7	
5*	S 255	06 09 48.4	18 01 40.2	—	6	
6*	S 254	06 10 03.4	18 10 34	36	—	
7*	S 269	06 10 40.2	13 49 02	18	—	
8*	S 269	06 10 56.6	13 56 57	39	—	
9*	S 271	06 11 07.7	12 32 51	13	—	
10*	S 271	06 11 25.4	12 25 09	12	—	
11*	S 271	06 11 34.9	12 19 47	26	—	
12	S 269	06 11 36	13 43 30	25	—	
13*	S 271	06 11 40.1	12 18 22	49	—	
14*	S 271	06 11 44.8	12 16 48	14	—	
15	S 269	06 11 48	13 46 12	15	—	
16*	S 271	06 12 13	12 20 34	08	—	
17*	S 271	06 12 16.2	12 10 21	20	—	
18*	S 271	06 13 29.5	12 21 08	33	—	
19*	S 271	06 13 34.6	11 57 03	465	—	4 CP11.22 (178 MHz: 4200 m.f.u.)
20	S 266	06 15 43.8	15 13 27.0	—	120	
21	S 266	06 16 05.8	15 18 21.6	—	5	
22	S 266	06 16 17.3	15 22 21.5	—	90	VRO 15.06.02 (610 MHz: 3500 m.f.u.)
Not Detected						
VRO 17.06.02		06 10 49	17 53 36	≤ 30	—	
VRO 18.06.02		06 11 13	18 18 24	≤ 75	—	

clumping factor f^2 is taken to be unity. The H II regions are assumed to be at an electron temperature $T_e = 10^4$ K and to have optically thin thermal spectra. The latter assumption is confirmed by the observations listed in Table 2.

² The clumping Factor f is defined as $\theta_{\text{total}}^3 / \theta_{\text{clump}}^3$. The electron density scales with $f^{1/2}$, the mass with $f^{-1/2}$.

The headings of Table 7 are self-explanatory. In the remainder of this section, I will discuss the individual H II regions. A comparison of the radio maps and optical photographs is possible after determination of accurate positions of stars near the nebulae. The positions were measured by A. A. Schoenmaker from the Palomar Sky Survey prints with the use of a Zeiss two-

Table 7. Derived parameters

Name	Assumed distance D (kpc)	Mean cylindrical diameter d (pc)	r.m.s. Electron density n_e (cm^{-3})	Peak emission measure (10^4 pc cm^{-6})	Optical Depth τ_{1415}	Mass (M_\odot)	Excitation parameter u (pc cm^{-2})
(1)	(2)	(3)	(4)	(5)	(6)	(7)	(8)
S 254	1.25	3.8	26	0.25	0.0004	28	19
S 256	1.25	0.40	230	2.1	0.0033	0.3	9
S 257	1.25	0.87	130	1.7	0.0026	1.8	14
G 192.58–0.04	1.25	≤ 0.02	≥ 7145	≥ 112	≥ 0.1760	≥ 0.04	3
G 192.60–0.04	1.25	0.05	900	5.0	0.0079	0.004	3
S 255	1.25	0.96	210	4.3	0.0068	3.6	19
S 258	1.25	0.26	≤ 180	≤ 0.7	≤ 0.0011	≤ 0.005	≤ 4
S 269 Total	2.0	1.14	125	2.0	0.0031	5.6	19
S 269 A	2.0	0.21	835	17	0.026	0.16	—
S 271	2.0	0.92	190	2.7	0.0042	1.45	14
S 272	2.0	0.15	285	1.4	0.0022	0.02	4
S 266	1.5	0.47	160	1.2	0.0019	0.3	8

dimensional measuring machine. The positions are given in Table 8 with respect to AGK 2 stars.

2. S 254 (G 192.51–0.15)

On the red Palomar Sky Survey print (Fig. 1) S 254 shows up as the largest of a group of H II regions. It measures almost 10 arc min across, but has a low optical surface brightness. Figures 2a and 2b show the λ 21 cm radio map, restored with synthesized beams of 20×65 arc s and 55×173 arc s respectively.

Planimetry yields in both maps the same total flux-density of 1.8 f.u. for S 254. The peak radio surface brightness is only $1.5 \cdot 10^{-25} \text{ erg cm}^{-2} \text{ s}^{-1} \text{ Hz}^{-1} \text{ arc min}^{-2}$ (15 m.f.u. per arc min squared). The r.m.s. electron

density of S 254 is low: only 26 cm^{-3} . The brightest radio area coincides with the optically brightest part. The r.m.s. electron density of this part may reach $50\text{--}65 \text{ cm}^{-3}$. The excitation parameter of 19 pc cm^{-2} indicates excitation by a B 0 or B 0.5 star (Churchwell and Walmsley, 1973; Panagia, 1973). Georgelin et al. (1973) list a 9^m8 exciting star (HD 253247) with spectral type O 9.5 V. According to Churchwell and Walmsley (1973) an O 9.5 V star has an excitation parameter of 41 pc cm^{-2} , while Panagia (1973) gives 31 pc cm^{-2} . Both values show S 254 to be mass-limited (Lyman continuum photons escape).

Nevertheless, a comparison of the positions and radial velocities of S 254, S 255 and S 257 with the Greenbank Maryland 21 cm line survey (Westerhout, 1969) shows that the regions occur in the vicinity of a neutral hydrogen maximum (Fig. 3).

If on the other hand S 254 were to be just photon-limited its exciting star would have to be of a later type than Georgelin et al. (1973) assume. The discrepancy which they note between the stellar distance of 3.2 kpc and the kinematical distance of 1.1 kpc would then vanish. A very accurate determination of the spectrum of HD 253247 might thus be worthwhile.

3. S 255 = IC 2162 (G 192.63–0.02)

This region is the brightest of the group S 254–S 258. Figure 4 shows a monochromatic H β photograph, adapted from Chopinet et al (1974).

This figure clearly shows the complicated structure of the nebula. The eastern part is much brighter than the western half. The two parts are separated by a dark band. The exciting star of magnitude $m_V = 11.7$ is located on the edge of the dark band. Chopinet et al. (1974) suggest that it is of a spectral type near B 0, which agrees well with the excitation parameter of 19 pc cm^{-2} derived from the radio observations. The radio structure at λ 21 cm is shown in Figures 2a and 2b; these figures

Table 8. Positions of stars near the observed regions measured by A. A. Schoenmaker

Number (1)	$\alpha(1950.0)$ (2)	$\delta(1950.0)$ (3)	Near (4)	Remarks (5)
1	06 ^h 09 ^m 26 ^s .7 \pm 0 ^s .1	+ 18 ^o 01' 46 ^s .9 \pm 1 ^s	S 254	Exciting star
2	06 09 41.1	17 57 15	S 256	Exciting star
3	06 09 54.6	18 02 29	S 257	
4	06 10 04.0	17 58 12	S 255	
5	06 10 08.8	17 59 33	S 255	Exciting star
6	06 10 13.4	18 01 08	S 255	
7	06 10 17.3	17 58 43	S 255	
8	06 11 36.6	13 49 20	S 269	
9	06 11 41.6	13 51 19	S 269	
10	06 11 51.9	13 52 08	S 269	
11	06 11 55.0	13 51 45	S 269	
12	06 11 57.3	13 49 54	S 269	
13	06 11 59.7	12 22 06	S 271	
14	06 12 00.0	12 19 08	S 271	
15	06 12 00.5	13 50 17	S 269	
16	06 12 02.5	12 19 04	S 271	
17	06 12 08.2	12 23 25	S 271	
18	06 12 11.8	12 21 59	S 271	
19	06 12 13.3	12 20 52	—	= S 272
20	06 15 53.5	15 18 09	S 266	Exciting star

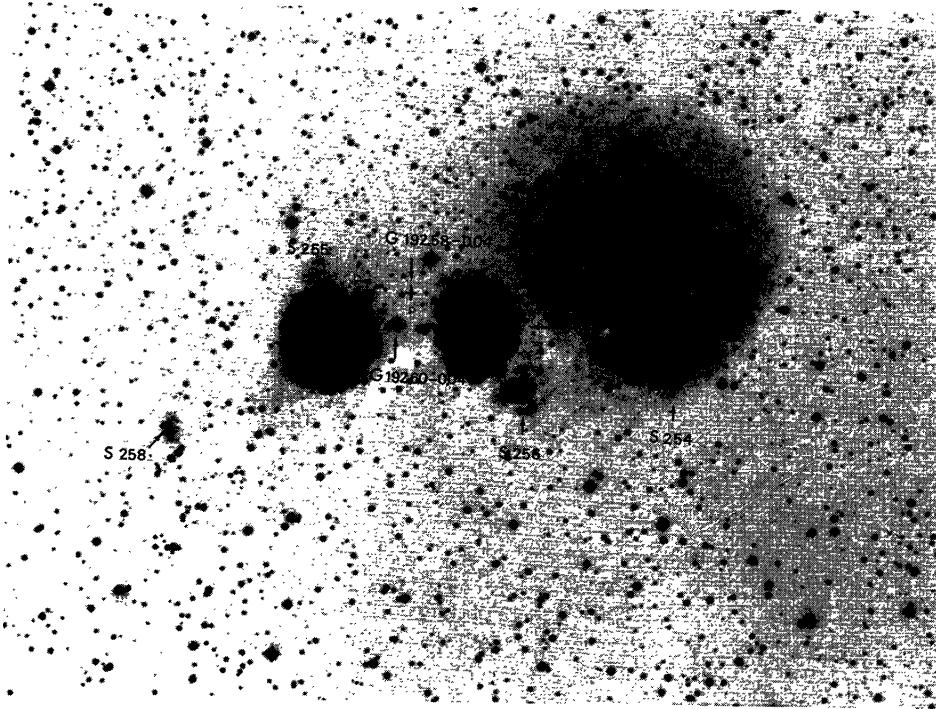


Fig. 1. Reproduction of the red Palomar Sky Survey print showing the group of H II regions S 254–S 258

also contain S 256, S 257 and two anonymous sources discussed later on.

Since the sources are not very much larger than the λ 21 cm beam, little structure is visible in this map. The λ 6 cm map, shown as Figure 5, is more detailed.

In general the radio structure of the eastern half resembles the optical structure roughly but not precisely.

It seems therefore, that both ionized gas and the obscuring dust in the eastern part of S 255 are distributed throughout the nebula in a very inhomogeneous way, on a typical scale of at most 5–10 arc s (corresponding to 0.03–0.06 pc at a distance of 1.25 kpc). The exciting star coincides almost, but not exactly, with the radio maximum (see Fig. 5).

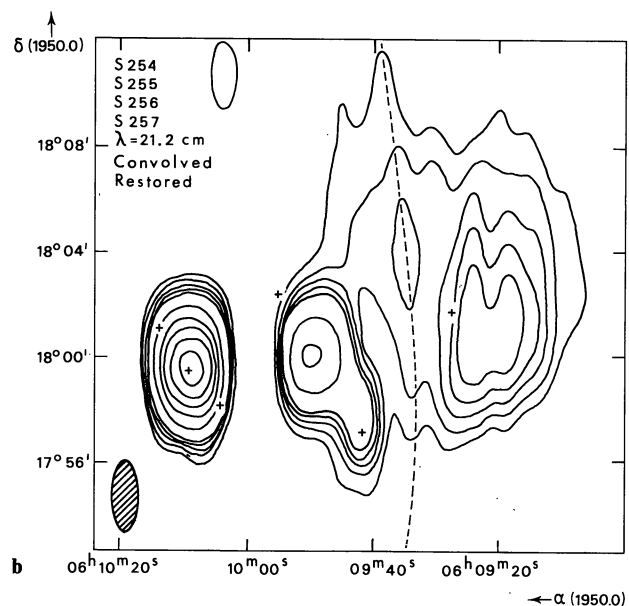
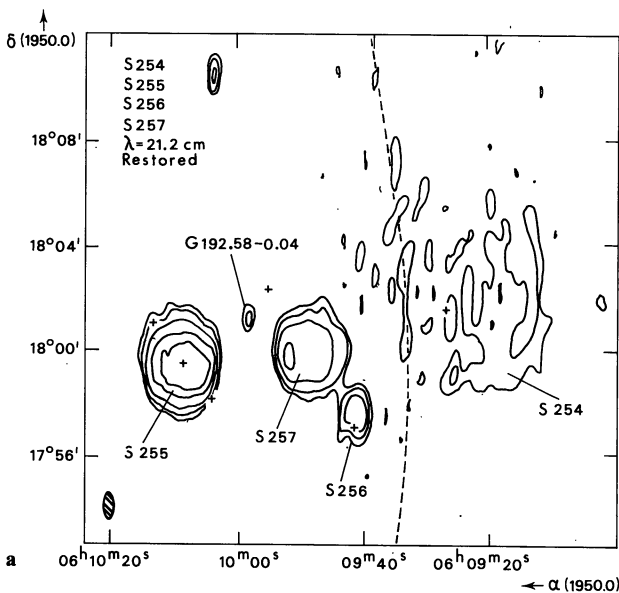


Fig. 2a and b. Observations at λ 21.2 cm of S 254–S 257. The crosses mark the positions of stars visible on Figure 1. The dashed line indicates the position of the first grating ring on S 255. Remnants of this grating ring are still present in the maps. (a) Synthesized beamwidth 20×65 arc s. Contour values 3.75, 7.50, 15, 30, 45 and 60 m.f.u. per synthesized beam area. (b) Synthesized beamwidth 55×173 arc s. Contour values 10, 20, 30, 40, 50, 100, 150, 200, 250 and 300 m.f.u. per synthesized beam area

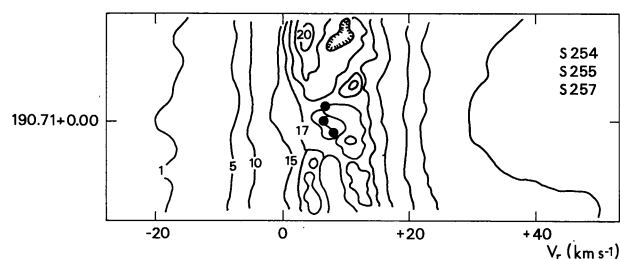


Fig. 3. Neutral hydrogen near S 254–S 257 (adapted from the Maryland-Greenbank survey). The group of H II regions (indicated by dots) is located near an H I maximum

The radio maximum is located on the edge of the dark lane, but the decrease in radio brightness is not nearly as steep as the decrease in optical brightness. Thus the absorbing dust will be at least partly in front of the nebula.

The optical brightness distribution peaks just east of the radio maximum. Chopinet et al. stress the presence of an optical brightness minimum around the exciting star. No evidence for such a feature is found at radio wavelengths. As indicated by Chopinet et al. (1973) the exciting star is in a region of maximum reddening

(E_{B-V} equals 1^m.1 for the star and varies from 0^m.4 to 1^m.0 for the nebula). It is probably significant that this position of maximum reddening is very close to the position of maximum radio brightness and presumably maximum gas density.

The radio measurements of the western half of the nebula show very little resemblance to the optical picture. It seems to suffer a larger amount of absorption than the eastern half of the nebula, in agreement with the conclusions drawn by Chopinet et al. (1974). Assuming that the depth of the radio peak region in the center of S 255 equals its diameter, one finds an r.m.s. electron density in the order of 350 cm^{-3} for the central region only. At the center electron densities were determined by Deharveng-Baudel (Chopinet et al., 1974) from the [S II] $\lambda 6724$ doublet; she finds a value near 1000 cm^{-3} . The mean value for most of the nebula is appreciably lower, probably less than 500 cm^{-3} . Since determinations of electron density using the [S II] doublet tend to favour the densest parts of the nebula, the clumping factor f will be at most $(1000/350)^2 = 10$. This in turn means that the mass of S 255 is overestimated at most by a factor of about 3 in Table 7. The ionized mass of S 255 will thus be between 3.6 and 1.2 solar mass.

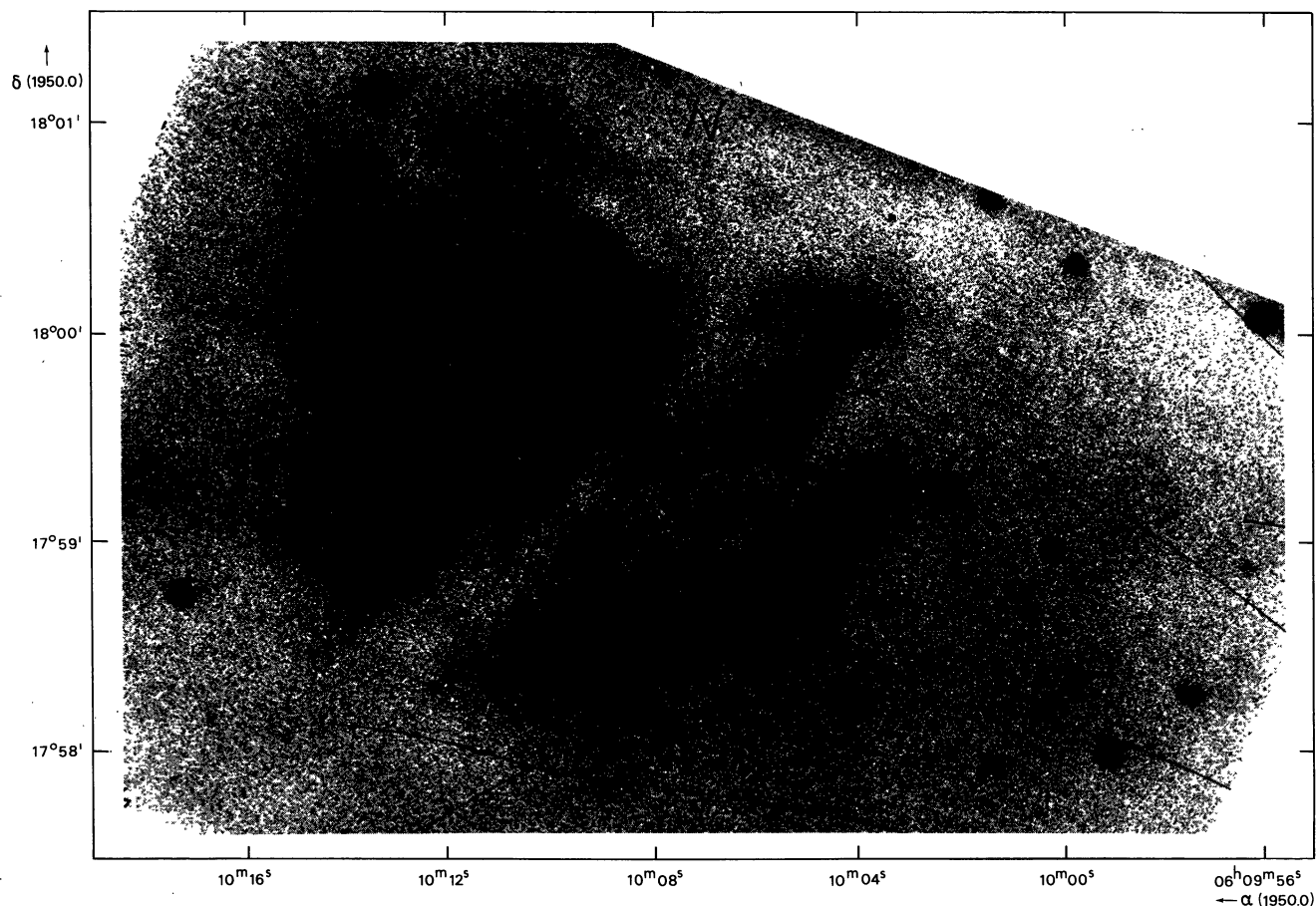


Fig. 4. H β photograph of S 255

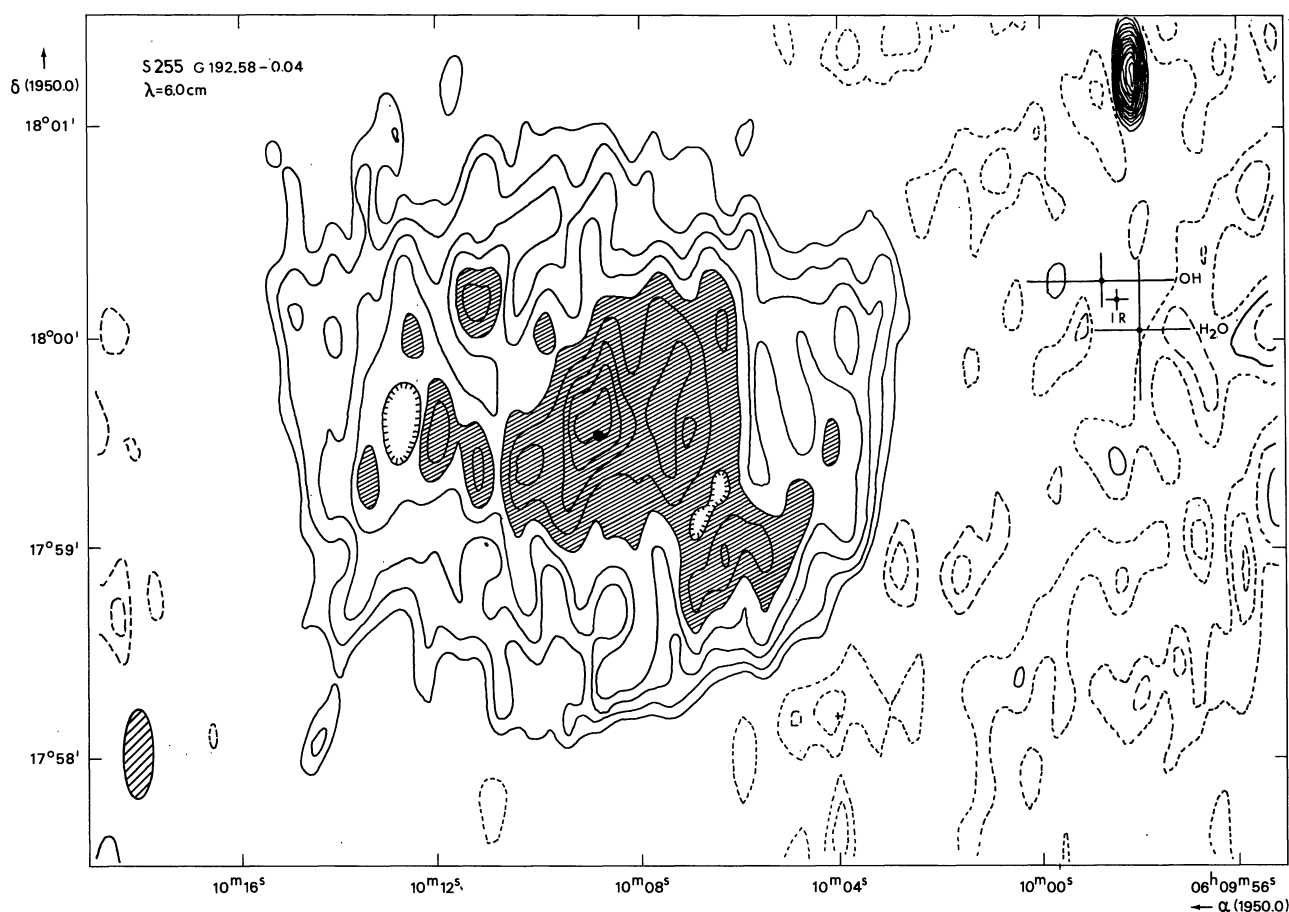


Fig. 5. λ 6.0 cm map of S 255. The positions of the H₂O and OH masers, and the infrared sources are indicated with the errors. The black dot indicates the position of the exciting star of S 255. Contour values 3, 4.5, 6, 7.5, 9, 10.5, 12, 13.5 and 15 m.f.u. per synthesized beam area

4. G 192.58–0.04 and G 192.60–0.04

Between S 255 and S 257 two small, weak radio sources are found. The brightest of the two (G 192.58–0.04) was also observed with the NRAO interferometer at λ 11 cm with $S_{2695} = 23$ m.f.u. and is less certain at λ 4 cm with $S_{8085} \approx 16$ m.f.u. (Lo, 1974). These data suggest a thermal spectrum becoming optically thick at 2000 MHz. Using this and the equations by Mezger, Schraml and Terzian (1969) I derive a (gaussian) angular diameter of 0.7 arc s, implying a (cylindrical) linear diameter of 0.005 pc or 1050 A.U. at a distance of 1.25 kpc. The r.m.s. electron density will be of the order of $n_e = 6 \cdot 10^4 \text{ cm}^{-3}$. At the position of the source, no optical emission is evident on the Palomar Sky Survey prints.

The other source (G 192.60–0.04) coincides with a small nebulosity on the red Palomar Sky Survey print with a size of about 10 arc s. In the same area, Lo and Burke (1973) discovered an H₂O maser source. The position of the OH maser found by Turner (1971) was determined with high accuracy by Evans et al. (1976); Beckwith and Evans (1976) also found a near-infrared source in the vicinity. The positions of the OH, H₂O and IR sources are indicated in Figure 5. The sources do

definitely not coincide with G 192.58–0.04, although that source has characteristics reminiscent of the radio continuum sources that Habing et al. (1974) generally find to be associated with OH maser sources. The projected linear distance between the maser source and the radio continuum source is about 0.5 pc.

G 192.60–0.04 lies within the error box of the OH maser position, but outside the error boxes of the IR and H₂O positions. The projected linear distance to the IR source is about 0.12 pc.

In the general direction of S 255 emission of CS was detected at 49000 MHz by Morris et al. (1974). Presumably this emission originates in the same area as the OH/H₂O emission. The presence of CS line emission indicates local densities in excess of 10^4 cm^{-3} . Such high densities are consistent with the density derived for S 192.58–0.04 and the total visual obscuration of that source. The CO cloud observed by Blair et al. (1975) likewise has its peak intensity near G 192.58–0.04.

5. S 256 (G 192.60–0.13)

Chopin et al. (1974) did not study S 256, but the nebula is faintly visible on a monochromatic H β photograph of S 257 (Fig. 6). The λ 6 cm radio map

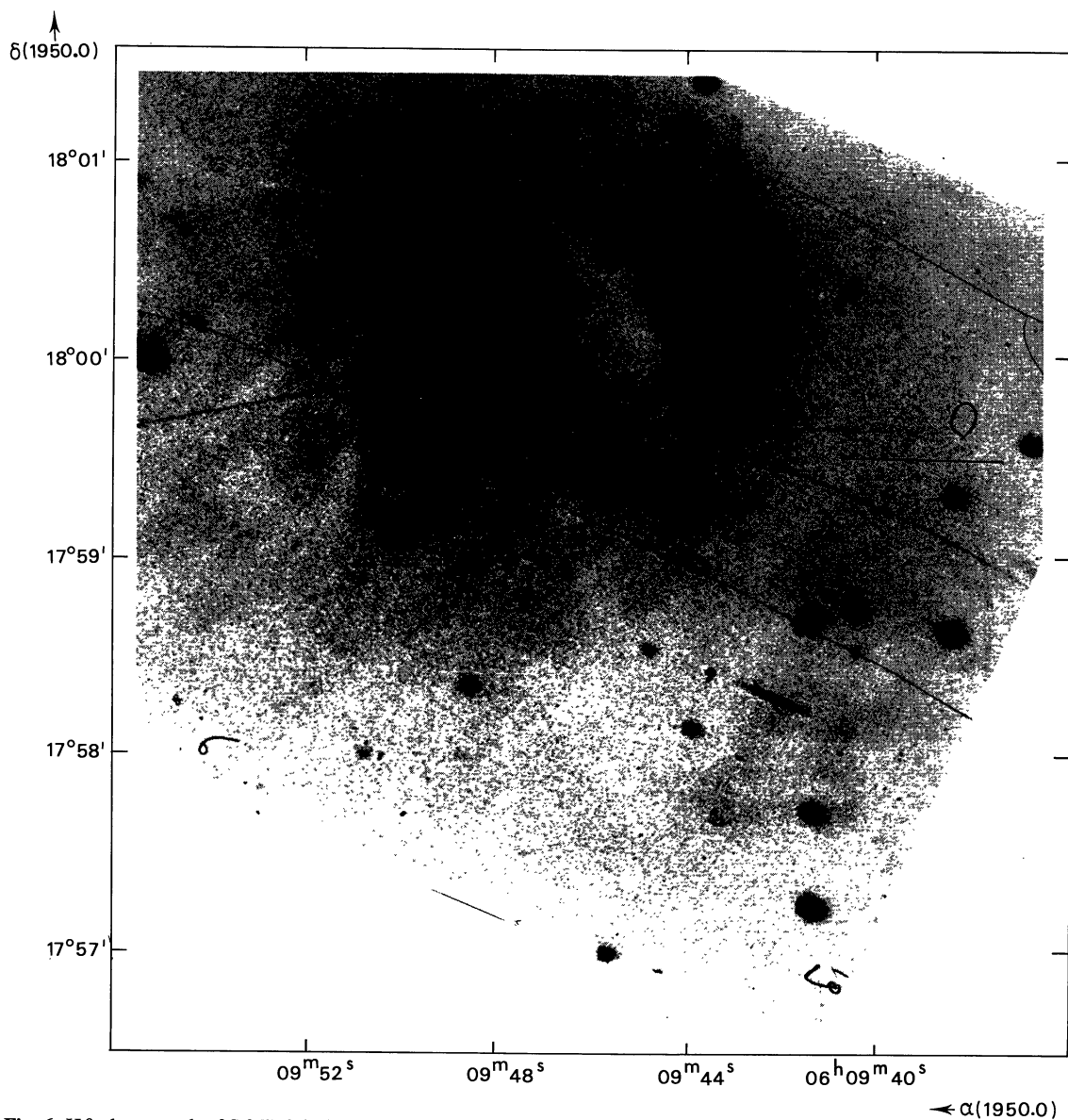


Fig. 6. H β photograph of S 257. S 256 is faintly visible in the lower right hand corner

(Fig. 7) reproduces the low brightness dip around the central star, but it also shows the western half much brighter than the eastern half and emission from the southeastern part. Thus obscuring dust is clearly determining the optical aspect of S 256 on a scale of 0.2 arc min (or about 0.1 pc). The $\lambda 6$ cm radio map gives the impression of a shell source with an uneven brightness distribution. The radio excitation parameter of 9 pc cm^{-2} indicates excitation by a B 0.5 V star. The central star of S 256 is appreciably weaker than that of S 257 (cf. Fig. 6) for which Chopinet et al. (1973) quote a visual magnitude of $+10^m.8$. From the Palomar Sky Survey print, I estimate the visual magnitude of the central star in S 256 to be of $+14^m$. The difference of 3^m is more than one would expect on the basis of spectral type difference, and it seems likely that the

star in S 256 is more reddened than the one in S 257. If the star in S 256 is of earlier spectral type than B 0.5 V, this increases the difference.

6. S 257 (G 192.58-0.08)

The nebula was studied at optical wavelengths by Chopinet et al. (1973, 1974). Optically, the nebula is divided into two parts by a dark band (Fig. 6). There are a few differences between the radio and the optical picture. The dark band is clearly due to obscuring dust, since the radio map does not show a similar gap. The radiostructure of the western part is unfortunately distorted by the presence of weak grating response to the bright nebula S 255 farther east whose position is indicated in Figure 7. Chopinet et al. (1974) find a small

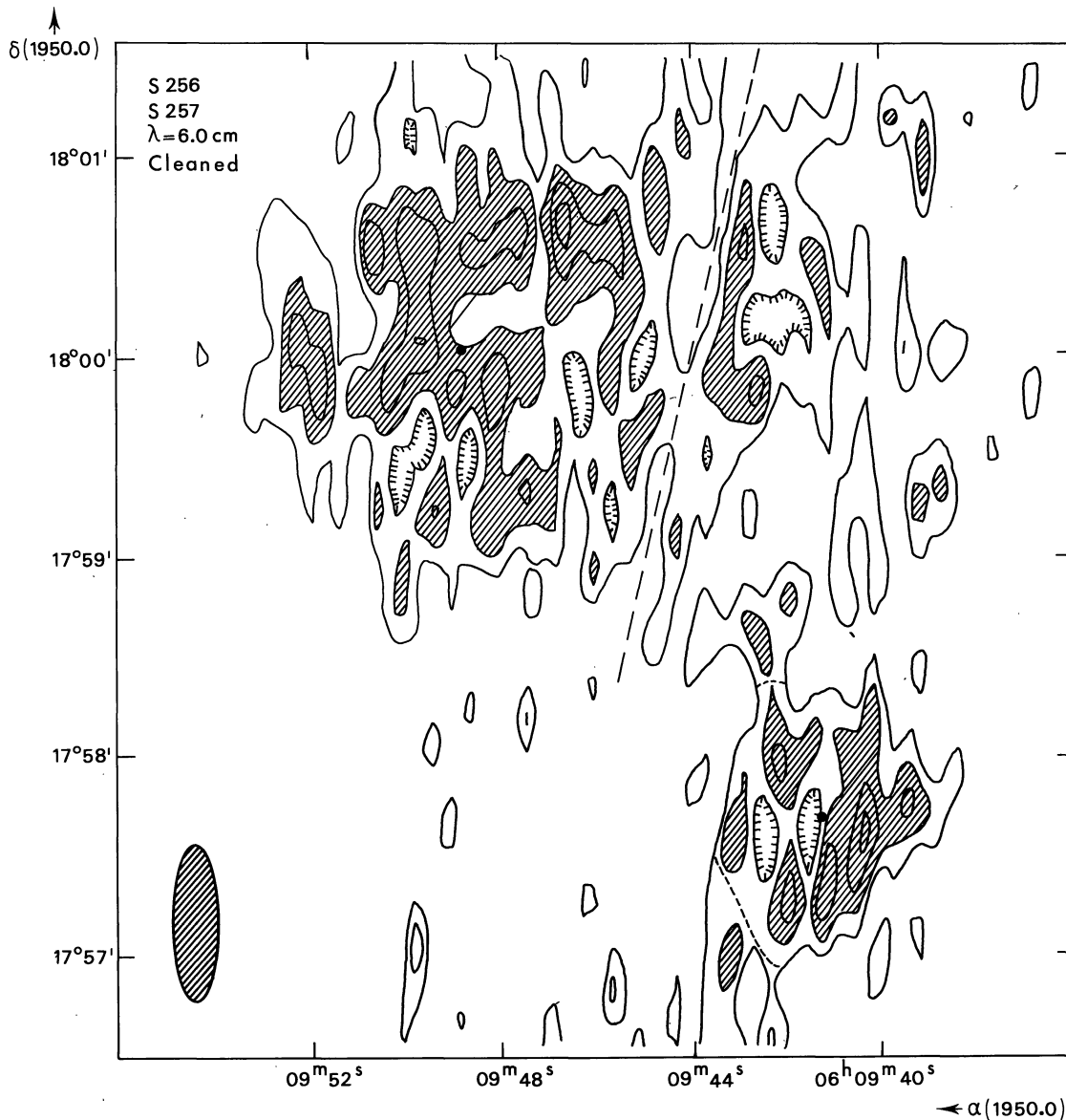


Fig. 7. λ 6.0 cm map of S 257 and S 256. The dots indicates the positions of the exciting stars. The remnant of a disturbing grating ring is marked by the dashed line. Contour values 1.5, 3, 4.5 and 6 m.f.u. per synthesized beam area

area of high density (marked A in their Figure 6) where the electron-density reaches a peak of about 1800 cm^{-3} . This area coincides with two strongly obscured peaks in the λ 6 cm map with sizes of about 8.5 arc s and flux densities of 4.5 m.f.u., yielding an r.m.s. electron density of 650 cm^{-3} for these two knots. Both in the eastern part and in the obscured central part small peaks are visible that presumably indicate condensations with electron densities of the order of 1000 cm^{-3} . For the whole nebula I find an r.m.s. electron-density of 130 cm^{-3} . The densities determined by Deharveng-Baudel from [S II] observations (Chopin et al., 1974) nowhere exceed 1000 cm^{-3} (except in point A) and are often less than 300 cm^{-3} . Thus one may conclude that essentially all structure in S 257 is resolved in the

λ 6 cm map, and that the clumping factor f is unlikely to be higher than 4 or 5. This means that the mass of S 257 is somewhere between 0.9 and $1.8 M_{\odot}$. The radio excitation parameter of 14 pc cm^{-2} indicates excitation by a B 0–B 0.5 star. Chopinet et al. (1973) list the spectral type of the exciting star HD 253327 as BOV. Such a star would have an excitation parameter of 31 pc cm^{-2} (Churchwell and Walmsley, 1973) or 22 pc cm^{-2} (Panagia, 1973) so that S 257 could well be mass-limited (density-bounded).

7. S 258 (G 192.74–0.04)

More than 2.5 pc southwest of S 255 a very small nebulous patch is visible on the red Palomar Sky Survey

print (Fig. 1) around a 15^m star. The optical size of the nebulosity S 258 is 0.6 arc min, (0.2 pc at a distance of 1.25 kpc). It is not found in the $\lambda 21$ cm radiomap. Its optical size and the upper limit to its flux density give an upper limit of 180 cm^{-3} to its r.m.s. electron density. This is a value similar to that of other H II regions in the same area. Its excitation parameter is less than 4 pc cm^{-2} , indicating excitation by a B 1 V star or a star of later type.

8. S 266 (G 195.64–0.10)

The flux density of S 266 found at $\lambda 6$ cm is appreciably lower than previously determined single dish values (Table 2). However, Higgs (1971) already noted a probable confusion of the source with VRO 15.06.02, which has a flux density of 3.5 f.u. at $\lambda 49$ cm and is situated 7.2 arc min to the northeast of S 266. At $\lambda 6$ cm this source is still visible with a flux density of about 90 m.f.u. (source $\neq 22$ in Table 6). At $\lambda 6$ cm two other sources with flux densities of 120 m.f.u. ($\neq 20$) and 5 m.f.u. ($\neq 21$) are also visible at distances of 5 arc min to the southwest and 3 arc min to the east respectively. Very probably all observations of S 266 listed in Table 2 are confused with these sources, this effect being most severe at low frequencies.

The only exception to this is the measurement at $\lambda 2.8$ cm with the 100 m Effelsberg dish which yields 56 m.f.u. (Altenhoff et al., 1975), in good agreement with the $\lambda 6$ cm WSRT value. In view of the low radio luminosity of S 266, Rubin's (1970) negative result is not surprising.

The nebula is often listed as a planetary nebula (PK 195–0.1, VV 42; cf. Chopinet and Lortet-Zuckermann, 1972). It is probably an H II region, since it resembles the other H II regions in this part of the galaxy rather closely. Frogel et al. (1972) arrived at the same conclusion on the basis of infrared observations. In their discussion of the infrared emission from S 266, they present two possible models: one in which the infrared emission is optically thin free-free emission from a gas at $T_e = 3500$ K and one in which the infrared emission originates in a number of optically thin dust shells at different temperatures. Clearly, the low observed radio flux density rules out the first model since the observed $S(10 \mu\text{m})/S(6 \text{ cm})$ ratio is at least 10, while a much lower value (~ 0.5) would be expected if both the infrared and the radio emission came from the same emitting gas.

In the second case, Frogel et al. (1972) expect the exciting star to be an early B or late O star, which is consistent with the radio excitation parameter of 8 pc cm^{-2} . Such a value is characteristic for a B 0.5 V star. The exciting star is included as MWC 137 in lists of stars with excess H α emission. Altenhoff et al. (1975) tentatively regarded it as a radio star on the basis of their $\lambda 2.8$ cm detection. However, both the H α emission

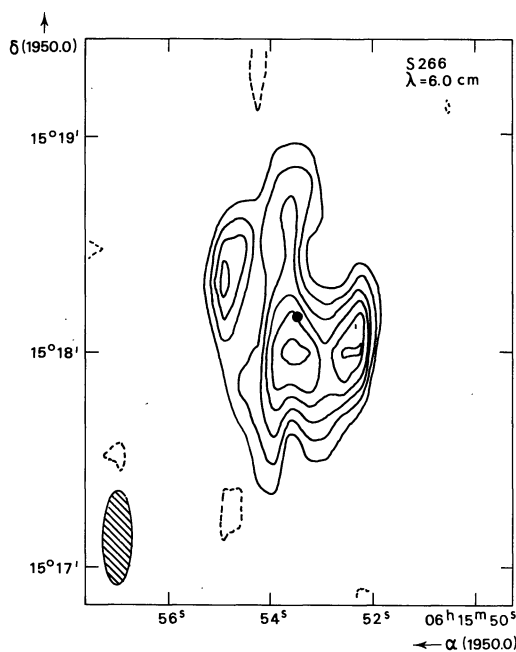


Fig. 8. $\lambda 6.0$ cm map of S 266. The position of the exciting star is marked by a dot. Contour values 2, 3, 4, 5, 6 and 7 m.f.u. per synthesized beam area

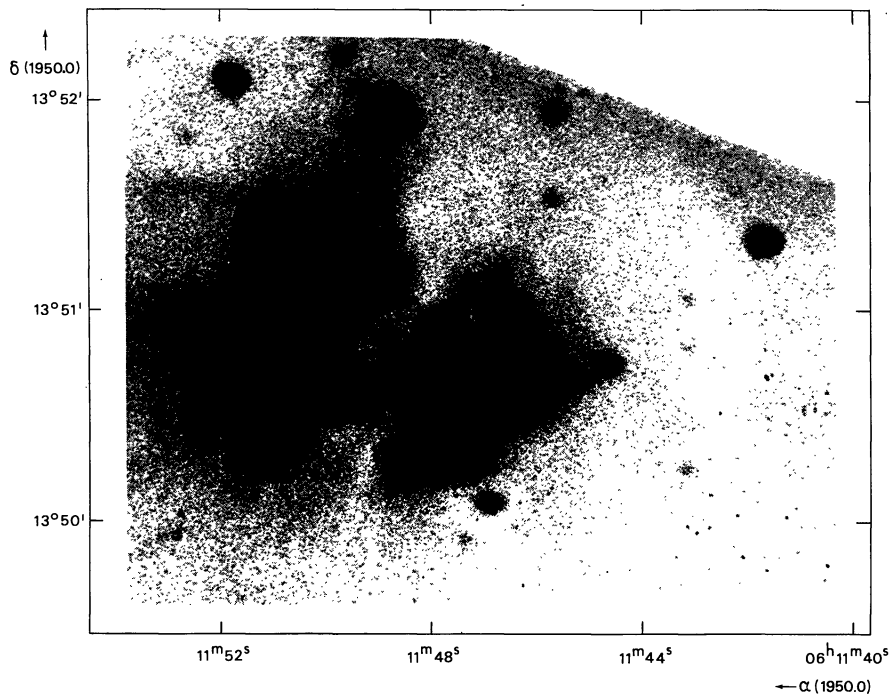
and the radio continuum emission are almost certainly entirely due to the ionized gas and dust of the nebula S 266, and not to the star. It should be remarked that on the red Palomar Sky Survey print, the object shows a wispy structure similar to the radio picture.

The radio map (Fig. 8) shows the nebula to contain three radio condensations with typical sizes of 10 to 30 arcs, corresponding to 0.07–0.22 pc (15000–45000 AU) at a distance of 1.5 kpc. The r.m.s. electron densities of these clumps are of the order of 400 – 800 cm^{-3} as compared with the r.m.s. density $n_e = 160 \text{ cm}^{-3}$ for the nebula as a whole. The peak emission measure of the condensations is about 4 – $5 \cdot 10^4 \text{ pc cm}^{-6}$. Taking into account the observed clumpiness at $\lambda 6$ cm, one finds an actual ionized mass of about 0.1 – $0.15 M_\odot$, only a small fraction of the mass of the exciting B star.

9. S 269 (G 196.45–1.67)

Figure 9 shows an H β photograph adapted from Chopinet et al. (1974). The $\lambda 6$ cm and $\lambda 21$ cm radio maps are given in Figures 10 and 11. The optical nebula is divided into two parts by a dark band. Chopinet et al. find electron-densities up to 1800 cm^{-3} . The radio data yield an r.m.s. electron-density of 200 cm^{-3} for the western part, and an r.m.s. density of 835 cm^{-3} for the radio peak S 269 A which has a size of 0.2 pc.

In view of the conclusion by Chopinet et al. (1974) that the nebula is rather uniformly reddened ($E(B-V) = 0.7$) one would expect good agreement between the radio and optical picture. The opposite is true.

Fig. 9. H β photograph of S 269

S 269 A does not have a counterpart in the H β picture. However, since the synthesized beam is elongated in a north-south direction due to the low declination of the source, it might consist of two, barely resolved components. These would then have r.m.s. electron densities of the order of 2000 cm^{-3} . The southernmost would more or less coincide with the bright optical patch in the south of the nebula, while

the northernmost component would be obscured by the dark band that divides the nebula in two.

In the direction and at the velocity of S 269, Wilson et al. (1974) found CO line emission (Table 1). From the $^{13}\text{C}^{16}\text{O}$ observations, they derive a column density $N_{\text{CO}} = 1.5 \cdot 10^{18} \text{ cm}^{-2}$.

If $N_{\text{CO}}/A_{\text{V}} = 1.6 \cdot 10^{17} \text{ cm}^{-2}$ (Encrenaz et al., 1975), this implies $A_{\text{V}} \approx 10^m$ for the CO feature.

Taking $n_{\text{H}} = n_{\text{e}} (\text{peak}) = 2000 \text{ cm}^{-3}$ as a typical value for the spatial density, one derives a thickness of about 4 pc for the obscuring dust layer. The actual density may however be higher implying a lesser depth for the obscuring dust cloud. Two smaller radiopeaks in the western part of the source, embedded in weak diffuse emission, do not coincide with the optical nebula but lie just north of it. Thus there seems to be an extended dust cloud just north of S 269.

Wynn-Williams et al. (1974) found a weak, extended (size 5–10 arc s) infrared source at $1.65 \mu\text{m}$ and $2.2 \mu\text{m}$, near and possibly coincident with the bright optical patch in the south.

In the direction of S 269, Turner (1971) discovered an OH emission source; an accurate position was determined by Wynn-Williams et al. (1974). Lo and Burke (1974) discovered an H $_2$ O maser at a slightly different position. The OH, H $_2$ O maser and IR positions are marked in the $\lambda 6 \text{ cm}$ map. They are located at the southern edge of the bright radiopeak. The H $_2$ O position coincides with the bright optical patch, the OH position is likewise within the bounds of the optical nebula. Surprisingly, both sources seem to be occurring at positions of relatively low obscuration. Neither of the two sources coincides with a definite

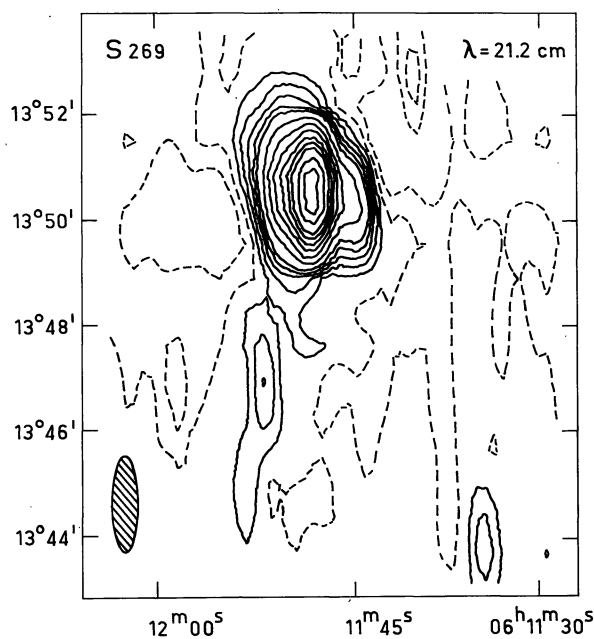


Fig. 10. $\lambda 21.2 \text{ cm}$ map of S 269 and sources # 12 and # 15. Contour values 5, 10, 15, 20, 25, 37.5, 50, 62.5, 75, 87.5, 100, 125 and 150 m.f.u. per synthesized beam area

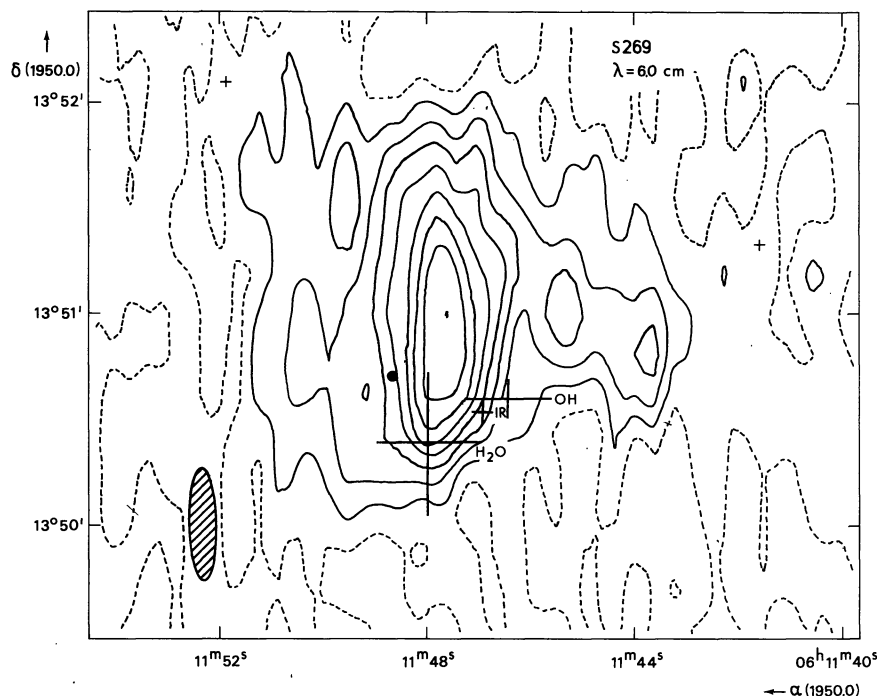


Fig. 11. λ 6.0 cm map of S 269. The dot marks the position of the exciting star. The position of the H₂O and OH masers and the infrared source is marked with the errors. Contour values 2.5, 5, 7.5, 10, 12.5, 15, 17.5 and 20 m.f.u. per synthesized beam area

radio feature, but this might be due to the effect of finite resolution. However the CO cloud found by Blair et al. (1975) has its central position in the same area. The dust cloud probably extends behind the optical nebula. CS emission was searched for, but not found by Morris et al. (1974). The radio excitation parameter of 19 pc cm^{-2} indicates excitation of S 269 by a B0 or a B0.5 star. S 269 is also found near a local maximum in the H I distribution (Fig. 12) in the Greenbank-Maryland Survey (Westerhout, 1969).

10. S 271 (G 197.78–2.32)

This nebula is often regarded as a planetary nebula, designated PK 197–2.1 (Chopin et al. 1972). It is probably an H II region on the basis of its appearance and derived physical parameters. The radio excitation parameter of 14 pc cm^{-2} indicates excitation of S 271 by a B0.5 star.

The radio structure (Figs. 14, 15) agrees fairly well with the optical appearance of the nebula (Fig. 13).

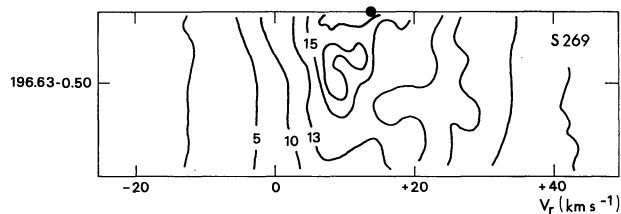


Fig. 12. Neutral hydrogen near S 269 (adapted from the Maryland-Greenbank survey). S 269 (indicated by a dot) is located near an H I maximum

There is a bright semi-circular shell in the east and south, and much weaker emission in the west and north.

In the bright shell, the r.m.s. electron density must be about 700 cm^{-3} , as compared with an r.m.s. density of 190 cm^{-3} for the whole nebula. The λ 6 cm radio map implies the presence of a band of obscuration across the nebula in a north to west direction; the central star is located in this band. The star is also on the edge of the radio maximum. It is near, but not coincident with a brightness minimum in both the radio and the optical picture.

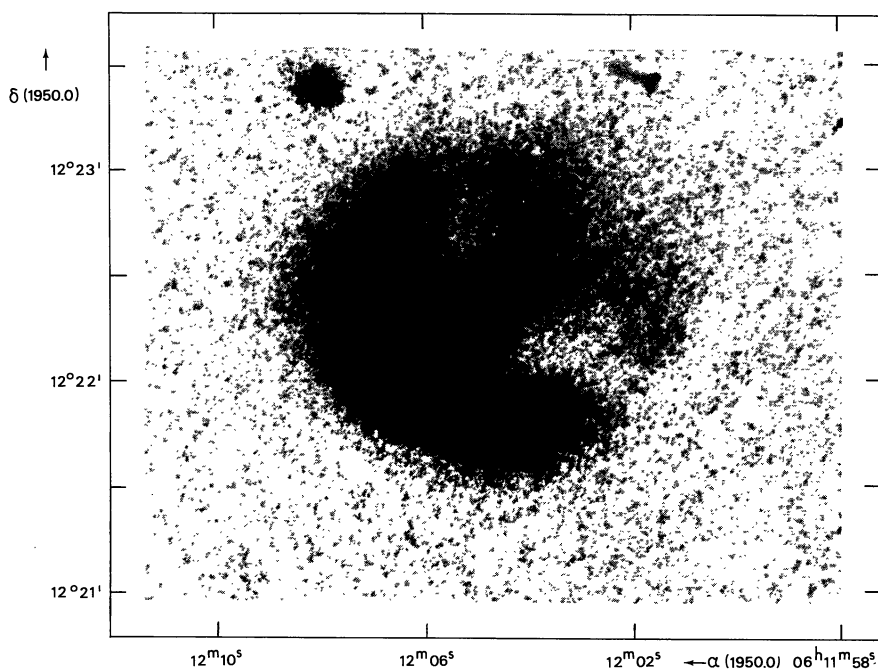
11. S 272 (G 197.83–2.31)

In the same field as S 271, and 3 arc min to the southwest of that object, a weak radio source with $S_{1415} = 3 \pm 1$ m.f.u. is found to coincide with the weak nebulosity S 272 (Fig. 14). Combined with an optical size of 0.3 arc min this flux density leads to an r.m.s. electron density of the same order as these found for the other H II regions in this part of the sky. The excitation parameter of 4 pc cm^{-2} permits excitation by even a B2 star.

IV. General Discussion and Conclusion

1. Star Formation in the Perseus Arm

The radial velocities of the regions studied (Table 1) shows that they all lie in the Perseus Arm, spread out over a length of 300 pc. In the same area four more H II regions (S 259, S 261, S 267 and S 268) that were not studied belong to the Perseus Arm (Fig. 16). Felli and Churchwell (1972) observed S 261 and S 268, while

Fig. 13. $H\beta$ photograph of S 271

S 267 is listed by Higgs (1971). The flux-densities of these regions indicate that they are excited by stars of spectral type O 9, O 9.5 and B 0.5 respectively. They all have r.m.s. electron densities of $10\text{--}20\text{ cm}^{-3}$, and thus resemble S 254 in these characteristics.

An inventory of the Perseus Arm between $l = 190^\circ$ and $l = 200^\circ$ therefore yields twelve optically visible H II regions, at least one obscured H II region, and at least two $\text{H}_2\text{O/OH}$ sources associated with these. None of the regions is excited by a star of spectral type earlier than O 9.5. The lack of early type O stars in these regions, and the general aspect of the area on the

Palomar Sky Survey prints (no widespread diffuse emission no large dust lanes) seem to suggest that in this part of the Perseus Arm no neutral cloud complexes massive enough to form star clusters containing early type O stars have been present for some time. Star formation on a smaller scale is still going on, viz. the two compact regions. It is of interest to note that one finds in the same direction as the observed H II regions ($l = 187.4\text{--}190.8$, $b = -2.1\text{--}+4.8$) and at the same distance ($D = 1.5\text{ kpc}$) the Gem OB 1 association (IAU Transactions XIIB, p. 348). The association contains seven B stars and only one O star (Morgan et al., 1953).

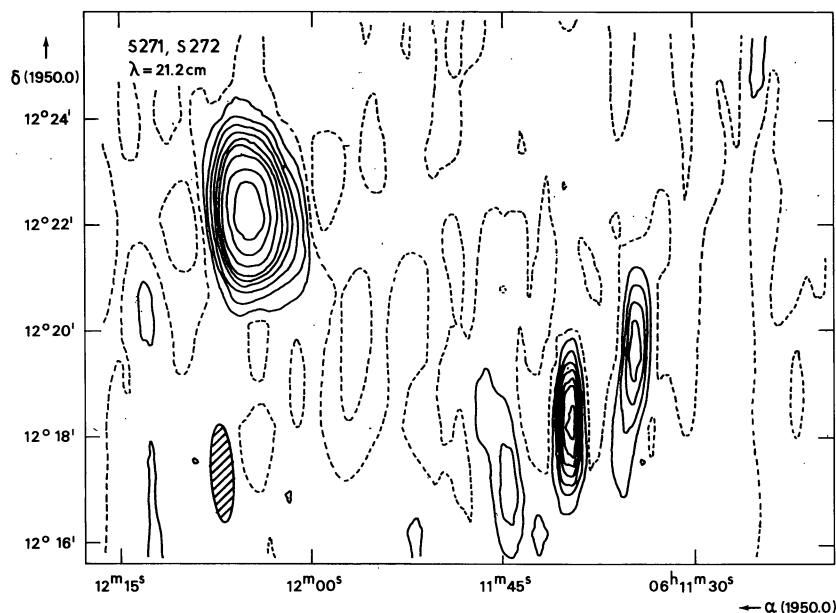


Fig. 14. $\lambda 21.2\text{ cm}$ map of S 271 and S 272. Sources # 11, 13 and 14 are also visible. Contour values 5, 10, 15, 20, 30, 37.5, 50, 62.5, 75 and 100 m.f.u. per synthesized beam area

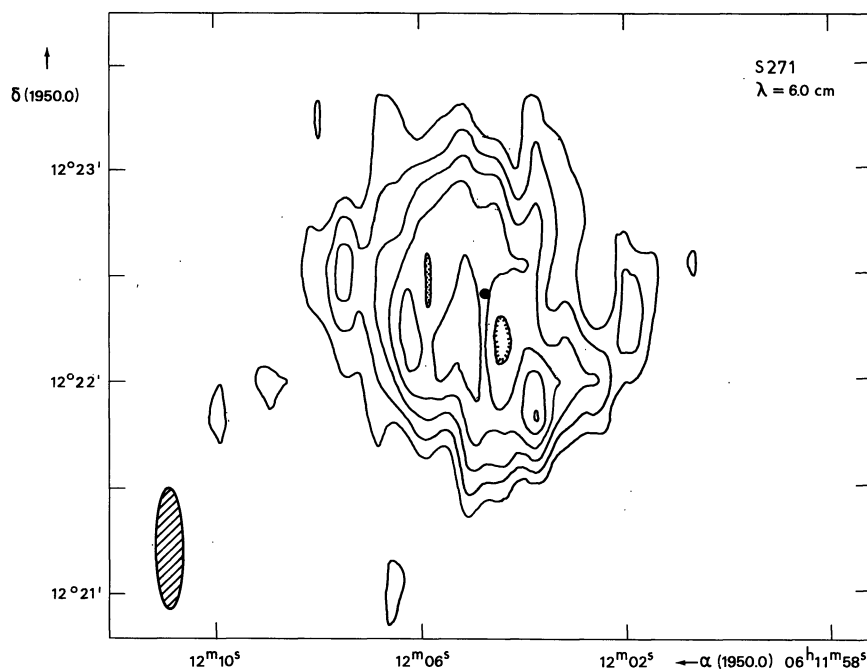


Fig. 15. λ 6.0 cm map of S 271. The dot marks the position of the exciting star

The O star is classified O 6.5 V by Conti and Alschuler (1971). This is consistent with the idea of star formation on a small scale going on in this part of the Perseus Arm. The situation in the anticenter region is in strong contrast with that around $l=70^\circ$ where apparently a massive, rich OB association is coming into being on the inside of the Perseus Arm (Paper II), and that around $l=111^\circ$ (Paper I) where a less massive, less rich OB association nevertheless appears to contain a relatively large number of early type O stars in a shorter section of the arm. The exciting stars of the H II regions in the anticenter region of the Perseus Arm appear to have formed completely independently from each other, since they are not connected to each other by molecular cloud complexes, diffuse emission or dust bands. The only exception is the group S 254–S 258 where at least seven early B stars in an area 3 arcs across are in the process of forming a new OB cluster.

2. Mass and Structure of the Regions

Most of the regions studied in this paper have r.m.s. densities in the range of $100\text{--}300\text{ cm}^{-3}$ and diameters of the order of $0.5\text{--}1.0$ pc, so that they cannot be classified as young, compact H II regions nor as old evolved H II regions. They are in an intermediate class with a dynamical age of at least 10^5 years. Comparison of optical [S II] observations and the radio observations show that in all cases the clumping factor is less than ten, and that it even may approach unity.

The estimated clumping factors yield new values for the ionized mass of S 255, S 257 and S 269. These are 1.2 , 0.9 and $1.1 M_\odot$ respectively. With the exception of

S 254, all regions studied appear to have an ionized mass of the order of $1 M_\odot$ or less.

All regions except the four smallest appear to be excited by a BO or B 0.5 star, which has a mass of about $10\text{--}15 M_\odot$. Thus the mass of ionized hydrogen around these exciting stars is about 10% of the stellar mass. If the exciting stars are not isolated single stars, but merely the brightest members of small clusters, the difference between the stellar mass and the ionized mass is even greater.

Can there be a large amount of gas in or next to these H II regions in a different form? As already mentioned, the differences between the radio picture and the optical picture strongly suggest the presence of dense clouds of dust and neutral gas in front of or inside several nebulae. The observations of Chopinet et al. (1974) and unpublished observations of Matthews (private communication) indicate the presence of dust inside and also near S 255, S 257 and S 269. From the $S(1415)/(H\beta)$ ratio's, $A_V=3^m$, while the reddening from $S(H\alpha)/S(H\beta)$ is $E_{B-V}=0^m7\text{--}0^m1$. The near-infrared observations of S 266 (Frogel et al., 1972) and S 269 (Wynn-Williams et al., 1974) likewise indicate dust mixed with the ionized gas. It is however unlikely, that the amount of neutral gas and dust inside the H II regions would exceed the amount of ionized gas. Also there are probably no thick, dense shells of neutral gas and dust around the regions for the following reasons: i) one would expect a higher extinction value and poorer visibility in that case; no obvious bright rims are seen; ii) comparison of the spectral type of the observed stars and the amount of radio emission of the regions suggest that most of these are mass-limited rather than photon-

limited; iii) there is no evidence of large scale dust clouds on the Palomar Sky Survey prints.

On a much larger scale, one does find large neutral hydrogen clouds as shown in the Greenbank-Maryland Survey (Westerhout, 1969), what one might expect in a region where star formation is still going on. In order to settle the question whether appreciable amounts of neutral matter really are absent from the observed regions, high resolution CO observations are of great importance. Should these confirm the picture sketched above, then one might tentatively suggest that at least the last stage in the process of star formation has a rather high efficiency, i.e. that most matter in the immediate vicinity of a protostar actually goes into it.

Acknowledgements. It is a pleasure to thank H. J. Habing and S. R. Pottasch for critical readings of the manuscript, L. L. E. Braes for doing part of the observations and reduction of the region S 266, and A. A. Schoenmaker for his accurate determination of star positions near the observed regions.

I also like to thank M. C. Lortet-Zuckermann, L. Deharveng-Baudel, K. Y. Lo, N. J. Evans, G. N. Blair and J. Matthews for kindly communicating their observations to me prior to publication.

The Westerbork Synthesis Radio Telescope is operated by The Netherlands Foundation for Radio Astronomy with the financial support of the Netherlands Organization for the Advancement of Pure Research (Z.W.O.).

References

- Altenhoff, W. J., Braes, L. L. E., Olton, F. M., Wendker, H. J.: 1975, in preparation
- Beckwith, S., Evans, N. J.: 1975, in preparation
- Baars, J. W. M., Hooghoudt, B. G.: 1974, *Astron. & Astrophys.* **31**, 323
- Blair, G. N., Peters, W. L., Vanden Bout, P. A.: 1975, *Astrophys. J. Letters* **200**, 164
- Casse, J. L., Muller, C. A.: 1974, *Astron. & Astrophys.* **31**, 333
- Caswell, J. L.: 1970, *Australian J. Phys.* **22**, 211
- Chopiniet, M., Lortet-Zuckermann, M. C.: 1972, *Astron. & Astrophys.* **18**, 166
- Chopiniet, M., Deharveng-Baudel, L., Lortet-Zuckermann, M. C.: 1974, *Astron. & Astrophys.* **30**, 233
- Chopiniet, M., Georgelin, Y. M., Lortet-Zuckermann, M. C.: 1973, *Astron. & Astrophys.* **29**, 225
- Churchwell, E., Felli, M.: 1970, *Astron. J.* **75**, 69
- Churchwell, E., Walmsley, C. M.: 1973, *Astron. & Astrophys.* **23**, 117
- Conti, P. S., Alschuler, W. R.: 1971, *Astrophys. J.* **170**, 325
- Day, G. A., Caswell, J. L., Cooke, D. J.: 1972, *Australian J. Phys. Suppl.* **25**
- Dickel, J. R., Young, K. S., McVittie, C. G., Swenson, G. W.: 1967, *Astron. J.* **72**, 757
- Ekers, R. D., Allen, R. J., Luyten, J. R.: 1973, *Astron. & Astrophys.* **27**, 77
- Evans, N. J., Crutcher, R. M., Wilson, W. J.: 1975, in preparation
- Encrenaz, P., Falgarone, E., Lucas, R.: 1975, in H II regions and Related Topics, Ed. T. L. Wilson and D. Downes, Springer Verlag, Heidelberg, p. 463
- Felli, M., Churchwell, E.: 1972, *Astron. & Astrophys. Suppl.* **5**, 369
- Ficarra, A., Padrielli, L.: 1968, *Nuovo Cimento* **57**, 478
- Frogel, J. A., Persson, S. E., Kleinmann, D. E.: 1972, *Astrophys. J.* **11**, 95
- Georgelin, Y. M., Georgelin, Y. P., Roux, S.: 1973, *Astron. & Astrophys.* **25**, 337
- Habing, H. J., Goss, W. M., Matthews, H. E., Winnberg, A.: 1974, *Astron. & Astrophys.* **35**, 1
- Higgs, L. A.: 1971a, Catalog of Radio Observations of Planetary Nebulae and Related Optical Data, Nat. Research Council Can. P. A. B. 1, no. 1
- Higgs, L. A.: 1971b, *Monthly Notices Roy. Astron. Soc.* **153**, 315
- Högbom, J. A.: 1974, *Astron. & Astrophys. Suppl.* **15**, 417
- Högbom, J. A., Brouw, W. N.: 1974, *Astron. & Astrophys.* **33**, 289
- Humphreys, R. M.: 1970, *Astron. J.* **75**, 602
- Israel, F. P., Habing, H. J., Jong, T. de.: 1973, *Astron. & Astrophys.* **27**, 143
- Israel, F. P.: 1976, *Astron. & Astrophys.* **48**, 193
- Jenkins, F. B., Savage, B. O.: 1974, *Astron. J.* **187**, 243
- Johnson, H. M.: 1974, in: H II regions and the Galactic Centre, 8th ESLAB Symposium ed. A. F. M. Moorwood, p. 103, ESRO SP-105
- Kaftan-Kassim, M. A.: 1968, quoted in: Higgs, 1971a
- Kazès, I., Le Squéren, A. M., Gadéa, F.: 1975, *Astron. & Astrophys.* submitted
- Lo, K. Y.: 1974, thesis Mass. Inst. Technology, Cambridge, Mass.
- Lo, K. Y., Burke, B. F.: 1973, *Astron. & Astrophys.* **26**, 487
- Mezger, P. G., Henderson, A. P.: 1967, *Astrophys. J.* **147**, 471
- Mezger, P. G., Schraml, J., Terzian, Y.: 1967, *Astrophys. J.* **150**, 807
- Miller, J. S.: 1968, *Astrophys. J.* **151**, 473
- Milne, D. K., Hill, F. R.: 1969, *Australian J. Phys.* **22**, 211
- Morgan, W. W., Whitford, A. E., Code, A. D.: 1953, *Astrophys. J.* **118**, 318
- Morris, M., Palmer, P., Turner, B. E., Zuckermann, B.: 1974, *Astrophys. J.* **191**, 349
- Panagia, N.: 1973, *Astron. J.* **78**, 929
- Rubik, N.: 1973, *Astron. J.* **78**, 929
- Rubin, R. H.: 1970, *Astron. & Astrophys.* **8**, 171
- Schmidt, M.: 1965, *Stars and Stellar Systems* **5**, 513
- Someren Greve, H. W. van: 1974, *Astron. & Astrophys. Suppl.* **15**, 343
- Terzian, Y.: 1966, *Astrophys. J.* **144**, 657
- Terzian, Y.: 1970, *Astron. J.* **75**, 1155
- Terzian, Y., Pankonin, V.: 1972, *Astron. J.* **77**, 115
- Thompson, A. R., Colvin, R. S.: 1967, *Astrophys. J.* **150**, 345
- Turner, B. E.: 1971, *Astrophys. Letters* **8**, 73
- Westerhout, G.: 1969, Maryland-Greenbank 21 cm line survey, 2nd Ed., University of Maryland
- Wilson, W. J., Schwartz, P. R., Epstein, E. E., Johnson, W. A., Etcheverry, R. D., Mori, T. T., Berry, G. G., Dyson, H. B.: 1974, *Astrophys. J.* **191**, 357
- Wynn-Williams, C. G., Becklin, E. E., Neugebauer, G.: 1974, *Astrophys. J.* **187**, 473
- Wynn-Williams, C. G., Werner, M. W., Wilson, W. J.: 1974, *Astrophys. J.* **187**, 41